

Reduction of the ordered magnetic moment in YMnO_3 with hydrostatic pressure

This article has been downloaded from IOPscience. Please scroll down to see the full text article.

2005 J. Phys.: Condens. Matter 17 L425

(<http://iopscience.iop.org/0953-8984/17/42/L01>)

View [the table of contents for this issue](#), or go to the [journal homepage](#) for more

Download details:

IP Address: 38.107.179.212

The article was downloaded on 21/02/2012 at 01:47

Please note that [terms and conditions apply](#).

LETTER TO THE EDITOR

Reduction of the ordered magnetic moment in YMnO_3 with hydrostatic pressure

M Janoschek^{1,2}, B Roessli¹, L Keller¹, S N Gvasaliya^{1,4}, K Conder³ and E Pomjakushina^{1,3}

¹ Laboratory for Neutron Scattering ETHZ and Paul Scherrer Institut, CH-5232 Villigen PSI, Switzerland

² Physik Department E21, TU München, 85748 Garching, Germany

³ Laboratory for Developments and Methods, Paul Scherrer Institut, 5232 Villigen PSI, Switzerland

Received 11 August 2005, in final form 16 September 2005

Published 7 October 2005

Online at stacks.iop.org/JPhysCM/17/L425

Abstract

YMnO_3 exhibits a ferroelectric transition at high temperature (≈ 900 K) and magnetic ordering at $T_N \approx 70$ K, where the dielectric constant shows an anomaly indicative of the magneto-dielectric effect. Here we report powder neutron diffraction experiments in this compound that show that the magnetic moment at saturation is reduced by application of hydrostatic pressure. Our results yield further insight about the nature of the spin–lattice interaction in ferroic materials.

1. Introduction

Yttrium manganite belongs to the family of rare-earth manganites RMnO_3 (R = rare earth element) which have both ferroelectric and magnetic order. These compounds crystallize in the hexagonal space group $P6_3cm$ below the paraelectric–ferroelectric phase transition ($T_C \sim 900$ K). The six Mn^{3+} magnetic moments in the unit cell are located in planes separated by ~ 5.7 Å along the hexagonal axis. In the $z = 0$ plane the Mn atoms are placed along the a , b and $-(a + b)$ axes, whereas in the $z = 1/2$ plane they are along the axes $-a$, $-b$ and $(a + b)$. The Mn atoms are centred in triangular bi-pyramids whose vertices are oxygen atoms. Because of the large distance between adjacent triangular layers, YMnO_3 is a good candidate for a geometrically frustrated two-dimensional antiferromagnet although small exchange interactions along the hexagonal axis drive magnetic ordering at $T_N \approx 70$ K. The magnetic structure of YMnO_3 was first studied by neutron diffraction by Bertaut [1], who found that two spin arrangements give similar agreement between observed and calculated powder diffraction patterns. Both models describe a triangular arrangement of the $S = 2$ magnetic moments in the basal plane with the coupling between adjacent layers being either ferromagnetic or

⁴ On leave from: Ioffe Physical Technical Institute, 26 Politekhnicheskaya, 194021, St Petersburg, Russia.

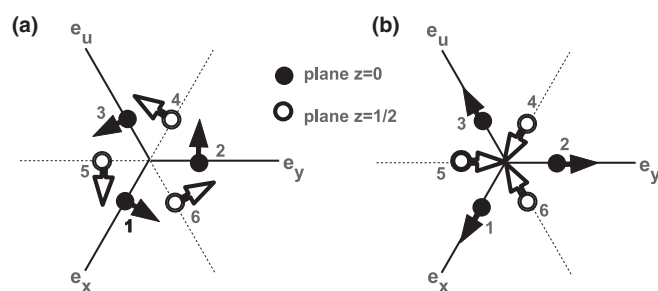


Figure 1. The two possible magnetic structures for YMnO_3 which are in agreement with neutron powder diffraction measurements. The configuration in the ab -plane is shown. (a) Structure defined by the irreducible representation Γ_1 ; the coupling between the layers $z = 0$ and $1/2$ is antiferromagnetic. (b) Structure defined by the irreducible representation Γ_3 ; the coupling between the layers $z = 0$ and $1/2$ is ferromagnetic and for this structure components of the moments perpendicular to the ab -plane (m_z) are possible. $m_{iz} = +m_z$; $i = 1, 2, 3$ and $m_{iz} = -m_z$; $i = 4, 5, 6$.

antiferromagnetic (further on labelled according to their irreducible representations Γ_3 and Γ_1 respectively; all representations are derived in [2]; see figure 1). Although both structures lead to very similar magnetic neutron intensities, Muñoz concluded from recent neutron diffraction studies that the probable magnetic structure of YMnO_3 corresponds to Γ_1 with the magnetic moment of the Mn ions being $\mu = 2.9 \mu_B$ at saturation [2]. The reduction of the value of the magnetic moment from the expected $4 \mu_B$ of Mn^{3+} free spins is taken as evidence that even in the ordered phase strong spin fluctuations are present due to geometrical frustration [3].

The RMnO_3 ferroics have received renewed interest since anomalies in the dielectric constant ϵ are found at the magnetic ordering temperature T_N [4], indicating a strong coupling between ferroelectric and magnetic properties. The origin of the magnetoelectric (ME) effect in these compounds is still not fully understood but spin–lattice interaction might play an important role in these materials. For example, anomalies of the structural parameters were reported at T_N that yield evidence that coupling between spin and lattice degrees of freedom is at the origin of the ME effect in YMnO_3 [5, 6]. In order to get more insight into the coupling between spin and structural parameters and their possible relationship with the magnetic and dielectric properties of ferroic materials, we investigated the influence of hydrostatic pressure on the magnetic ordering in YMnO_3 .

2. Experimental details

Polycrystalline YMnO_3 was prepared by a solid state reaction. Starting oxides of Y_2O_3 and MnO_2 with 99.99% purity were mixed and ground followed by sintering at $1000\text{--}1200^\circ\text{C}$ in air for 100 h with several intermediate grindings. The phase purity of the compound was checked with a conventional x-ray diffractometer (Siemens D500). The neutron measurements were performed at the neutron powder diffractometer DMC located at the cold source of the neutron spallation source SINQ. The instrument was operated with $\lambda = 2.566 \text{ \AA}$ and a PG filter was installed in the beam to remove higher-order harmonics. For measurements at ambient pressure, 13 g of polycrystalline YMnO_3 were filled in a standard vanadium container ($\phi = 15 \text{ mm}$). For the pressure experiments a clamp-type pressure cell was used, that can attain a maximum pressure of 15 kbar. Hydrostatic pressure is obtained by mixing the powder sample with Fluorinert. The effective pressure was calculated from the known pressure dependence of the lattice parameters of NaCl [7] that was mixed with the YMnO_3 sample. The sample was cooled in a ^4He cryostat of ILL type.

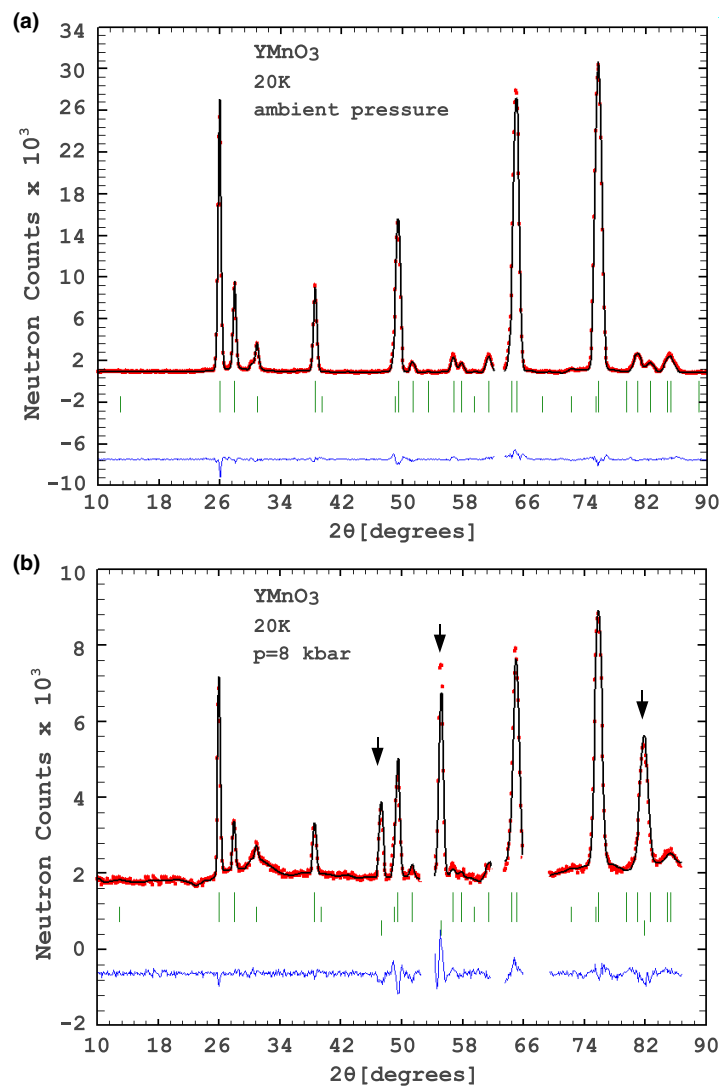


Figure 2. Observed (●) and calculated (—) neutron diffraction patterns of YMnO_3 at $T = 20$ K for (a) ambient pressure and (b) $p = 8$ kbar. The bars below the patterns denote the position of nuclear (upper row) and magnetic Bragg reflections (lower row). The diffraction pattern for $p = 8$ kbar contains additional reflections due to the NaCl powder (denoted by arrows). Bragg peaks originating from the pressure cell were excluded from the data. In addition, we note that the background is modulated around $2\theta = 28^\circ$, mainly due to the presence of Fluorinert in the neutron beam.

(This figure is in colour only in the electronic version)

3. Results and discussion

A first series of measurements was made at ambient pressure in the temperature range $1.5 \text{ K} < T < 300 \text{ K}$. A typical neutron diffraction pattern is shown in figure 2(a), that was analysed with the Rietveld method [8] implemented in the program FULLPROF [9]. The structural parameters found at $T = 300 \text{ K}$ are presented in table 1. The fit of the magnetic

Table 1. Results of the Rietveld refinement of neutron powder diffraction data for YMnO_3 at 300 K for ambient pressure and 9.6 kbar. Atomic positions: Y1 and O3 at 2a (0, 0, z); Y2 and O4 at 4b ($\frac{1}{3}, \frac{2}{3}, z$); Mn, O1 and O2 at 6c ($x, 0, z$) for Mn $z = 0$.

		Ambient pressure	9.6 kbar
a (Å)		6.15672(5)	6.14676(6)
c (Å)		11.4179(1)	11.4139(1)
v (Å ³)		374.802(4)	373.460(5)
Atomic positions			
Y1	z	0.26989(5)	0.27204(9)
Y2	z	0.22874(3)	0.2309(2)
Mn	x	0.3323(8)	0.337(2)
O1	x	0.31101(1)	0.3170(5)
	z	0.16069(3)	0.1474(1)
O2	x	0.63937(6)	0.6472(5)
	z	0.33703(3)	0.3399(1)
O3	z	0.47426(7)	0.4725(3)
O4	z	0.01401(5)	0.0132(3)
Agreement factors			
χ^2		8.13	5.01
Bragg-R-factor		1.734	5.085

structure of YMnO_3 was found to yield a slightly better agreement with the Γ_1 type (magnetic $R_{\text{Bragg}} = 4.68$, $\chi^2 = 5.57$) than the Γ_3 structure (magnetic $R_{\text{Bragg}} = 5.13$, $\chi^2 = 5.55$). We note that the symmetry of the Γ_3 structure allows the magnetic moments to have a component out of the ab -plane. However, agreement factors between observed and calculated intensities do not improve when spins are canted and we conclude that the magnetic moments lie in the hexagonal plane. With the Γ_1 structure, the value of the magnetic moment at $T = 1.5$ K is $3.09(2) \mu_{\text{B}}$, in good agreement with the results of Muñoz *et al.* The temperature dependence of the staggered magnetization is shown in figure 3.

Although the maximum load was applied to the pressure cell, we found that the effective pressure was 7.8 kbar at $T = 1.5$ K and increased to 9.6 kbar at $T = 300$ K. However, the pressure increased only slightly from 7.8 to 8.3 kbar in the temperature range $1.5 \text{ K} < T < 80$ K, where YMnO_3 is antiferromagnetically ordered. Figure 2(b) shows a typical neutron diffraction pattern measured at $T = 20$ K and $p = 8$ kbar. Apart from Bragg reflections of YMnO_3 , the diffraction pattern now contains additional reflections due to the NaCl powder. In addition, the background is high mainly due to the presence of Fluorinert in the neutron beam. Therefore, the statistical quality of the data is much reduced when compared with the results obtained at ambient pressure. The applied hydrostatic pressure mainly altered the lattice constant a whereas c remained almost unchanged ($\Delta a/\Delta c \approx 2.5$). The volume of the unit cell changed from $v = 374.802(4) \text{ Å}^3$ at ambient pressure to $v = 373.460(5) \text{ Å}^3$ at $p = 9.6$ kbar. Comparison of the structural parameters shown in table 1 indicates that only the z -coordinate of the O1 atom is significantly modified by application of pressure. The shift of the O1 atom decreases the length of the Mn–O1 bond from 1.84 to 1.68 Å. A preliminary analysis of the data at $T = 1.5$ K showed that the neutron diffraction peaks of YMnO_3 have very similar relative intensities as observed at ambient pressure. Least-square refinements of the diffraction pattern yielded good agreement factors for the magnetic structure with Γ_1 and Γ_3 symmetry, namely (magnetic) $R_{\text{Bragg}} = 9.95$ and $\chi^2 = 4.73$ for Γ_1 and (magnetic) $R_{\text{Bragg}} = 9.97$ and $\chi^2 = 4.78$ for Γ_3 respectively. Hence, the spin arrangement of YMnO_3 is not modified by hydrostatic pressure up to $p \sim 8$ kbar. However, the magnitude of the ordered magnetic moments is

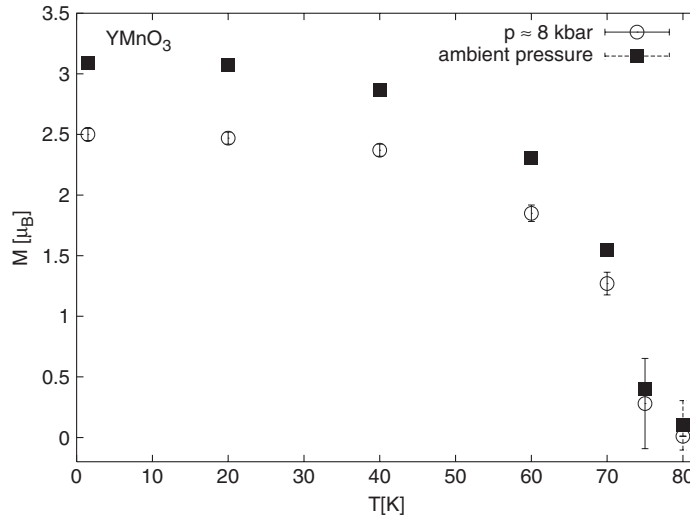


Figure 3. Temperature dependence of the magnitude of the Mn magnetic moments for ambient pressure and $p \sim 8$ kbar.

significantly reduced from $\mu \sim 3 \mu_B$ at ambient pressure to $\mu = 2.50(5) \mu_B$ at $p \sim 8$ kbar for the Γ_1 symmetry. We note that the ordered moment is reduced to $\mu = 2.44(5) \mu_B$ for magnetic structure with Γ_3 symmetry. The temperature dependence of the ordered magnetic moment is shown in figure 3. Although from neutron powder measurements it is difficult to determine the value of T_N precisely, we conclude from our data that the difference of the temperature of the phase transition from the paramagnetic to the ordered antiferromagnetic state is less than ~ 5 K at $p = 8$ kbar as compared to ambient pressure. A possible model to describe the magnetic and ferroelectric properties of ferroic materials was proposed by Gong *et al* [10] that includes antiferromagnetic Heisenberg exchange interactions and a double-well potential for the lattice displacements giving rise to ferroelectricity. The ME coupling is described by an interaction of the form $g_{\parallel} u_k^2 \mathbf{S}_{ai} \cdot \mathbf{S}_{aj}$ and $g_{\parallel} u_k^2 \mathbf{S}_{bi} \cdot \mathbf{S}_{bj}$ for the intraplane and $g_{\perp} u_k^2 \mathbf{S}_{ai} \cdot \mathbf{S}_{bj}$ for the interplane component respectively, where g_{\parallel} and g_{\perp} are the intra- and interplane ME coupling constants, u_k is the lattice displacement at site k , \mathbf{S}_{ai} is the Heisenberg spin operator, i and j denote the nearest neighbours to k and a and b represent the nearest planes. In the mean-field approximation, the ME coupling leads to a renormalization of the intra- and interplane exchange integrals J_{\parallel} and J_{\perp} to $J_{\parallel} + g_{\parallel} p^2$ and $J_{\perp} + g_{\perp} p^2$ respectively, where $p = \langle u_k \rangle$. In this approach, the Néel temperature is reduced by the ME coupling, but the value of the magnetic moment $\langle S^z \rangle$ in the ground state is essentially unaffected [11]. Although this is consistent with the observation that in HoMnO_3 the spin reorientation temperature T_{SR} of the manganese sublattice shifts to lower temperatures by about 1.5 K at $p \sim 8$ kbar [12], the model does not explain the moment reduction observed in YMnO_3 .

4. Conclusion

We investigated the influence of hydrostatic pressure on the properties of the magnetic ground state of YMnO_3 . The magnetic structure of YMnO_3 is found to have Γ_1 symmetry at $p = 8$ kbar. On the other hand, the ordered magnetic moment at saturation is significantly reduced by application of pressure. This suggests that coupling between the size of the magnetic

moment and the volume of the unit cell is important in ferroic materials and that application of hydrostatic pressure leads to an increase of the spin fluctuations in YMnO_3 and enhances the two-dimensional character of the magnetic properties of this compound. We suggest that application of pressure leads to a renormalization of the temperature dependence of the staggered magnetization, i.e. the strain influences the sublattice magnetization [13].

We thank D Sheptyakov for help and advice with the pressure cell and P J Brown for fruitful discussions. This work was performed at the spallation neutron source SINQ and was partially supported by NCCR MaNEP.

References

- [1] Bertaut B and Mercier M 1963 *Phys. Lett.* **5** 27
- [2] Muñoz A, Alonso J A, Martínez-Lope M J, Casáis M T, Martínez J L and Fernández-Díaz M T 2000 *Phys. Rev. B* **62** 9498
- [3] Park J, Park J-G, Jeon G S, Choi H-Y, Lee C, Jo W, Bewley R, McEwen K A and Perring T G 2003 *Phys. Rev. B* **68** 104426
- [4] Huang Z J, Cao Y, Sun Y Y, Xue Y Y and Chu C W 1997 *Phys. Rev. B* **56** 2623
- [5] Lee S, Pirogov A, Han J H, Park J-G, Hoshikawa A and Kamiyama T 2005 *Phys. Rev. B* **71** 180413
- [6] Sharma P A, Ahn J S, Hur N, Park S, Kim S B, Lee S, Park J-G, Guha S and Cheong S-W 2004 *Phys. Rev. Lett.* **93** 177202
- [7] Menoni C S and Spain I L 1984 *High Temp. High Pressures* **16** 119
- [8] Rietveld H M 1969 *J. Appl. Crystallogr.* **2** 65
- [9] Rodriguey-Carvajal J 1993 *Physica B* **192** 55
- [10] Gong S J and Jiang Q 2005 *J. Magn. Magn. Mater.* **285** 367
- [11] Zhong C G and Jiang Q 2002 *J. Phys.: Condens. Matter* **14** 8605
- [12] dela Cruz C, Yen F, Wang Y Q, Sun Y Y, Gospodinov M M and Chu C W 2005 *Phys. Rev. B* **71** 060407(R)
- [13] Mattis D C and Schultz T D 1963 *Phys. Rev.* **129** 175